

DOI: 10.1002/adfm.200700251

Control of Specular and Diffuse Reflection of Light Using Particle Self-Assembly at the Polymer and Metal Interface**

By Jin Soo Ahn, Troy R. Hendricks, and Ilsoon Lee*

We present a novel method of controlling the specular and diffuse reflection of light by the electrostatic deposition of a spherical particle monolayer followed by electroless plating. Charged polystyrene colloidal particles, ranging in size from 100 nm to 5 μm , were adsorbed from solution onto oppositely charged polyelectrolyte multilayers (PEM). The monodisperse particle monolayers were coated with nickel in a two-step electroless plating process using palladium catalysts. These surfaces can be used as diffusive metal reflectors with a uniformly controlled surface roughness due to the uniform size of deposited particles. In addition, the self-assembled particles at the polymer and metal interface deflected the internal stresses that build-up at the interface while the metal was being deposited. This allowed a thicker metal film to be deposited before delamination occurred. A UV-VIS spectrometer with movable fiber optic cables was employed to characterize the optical properties of the reflectors. The optical fibers permit versatile and precise measurements of specular and diffuse reflectance. By measuring the angular dependent reflectance, we demonstrate how to estimate the distribution of reflected light from the nickel coated surface and how to calculate the ratio of specular and diffuse reflection in the total reflected light. Optical measurements of our nickel samples showed that this approach could be used to control the portion of diffuse reflection from 8.25 to 59.97 %. Additionally, a quartz crystal microbalance was employed to study the electroless nickel plating rate on PEM. Our proposed method is simple, cost-effective and convenient for mass production because the process consists of a series of simple immersion steps without vacuum technology or special equipment.

1. Introduction

Diffuse reflectors are widely used in the back-light units of liquid crystal display (LCD) panels,^[1-4] light-emitting diodes (LED)^[5,6] and solar cell devices.^[7,8] A perfect diffuse reflector is matter that reflects incident light uniformly to all directions and can be observed from all angles. Manipulating topographical roughness on a highly reflective surface is a practical method to create a diffuse reflector. A uniform surface with a controlled surface roughness reflects incident light in a diffusive manner and reduces specular reflection by randomly scattering light in all directions.^[9-12] Controlling the ratio of specular and diffuse reflection is the most important aspect in the design of a diffuse reflector. Specific applications may require different ratios of specular and diffuse reflectance.

With their high reflectivity and low solar absorption, metals easily satisfy the general requirements for diffuse reflectors. The manipulation of a low-reflective metal surface by sputter coating metal has been reported.^[13] One advantage of this vac-

uum deposition process is that the surface roughness can be controlled in the process of forming the reflectors which eliminates an additional roughening step. However, the process requires a high vacuum that is costly to produce and not suitable for mass production.

To meet the higher industrial requirements of most current applications, metal reflectors are required to be heterogeneous or multilayered with additional materials. These additional modifications include incorporating brightening agents,^[14,15] multilayering or over-coating,^[16] and protective coating.^[17,18] Metal reflectors formed by electroless deposition are more cost-effective and efficient starting point when additional modifications are required. Among the highly reflective metals, nickel is one of the most common and inexpensive materials formed by electroless deposition and has moderate reflectivity over many wavelengths (Fig. 1).^[19] For nickel, the coefficient of absorption of solar radiation is 0.15. This value exceeds the value for gold or steel and is equivalent to that of aluminum.^[20] For specific applications when the nickel reflectivity is less than what is required, coating the nickel with another substance such as silver can provide 'better optical brightness (or reflectance)'. This over-coating scheme will eliminate the need for a thick layer of expensive materials such as silver. The design of metal reflectors can be optimized with a combination of the proper metallization technique and selection of the materials to be coated.

Using an electroless plating technique to create a diffuse reflector will be cost efficient and suitable for mass production if the surface roughness of the deposited metal can be controlled

[*] Prof. I. Lee, J. Soo Ahn, T. R. Hendricks
Department of Chemical Engineering and Materials Science
Michigan State University
East Lansing, Michigan-48824 (USA)
E-mail: leeil@egr.msu.edu

[**] We would like to acknowledge Dr. Michael F. Rubner and Prof. Paula T. Hammond at MIT for the discussion of the work. This work was funded by the NSF (CTS-0609164), the AFOSR (Air Force Equipment Grant No. FA 9550-06-1-0417), the Michigan Economic Development Corporation, and the MSU foundation.

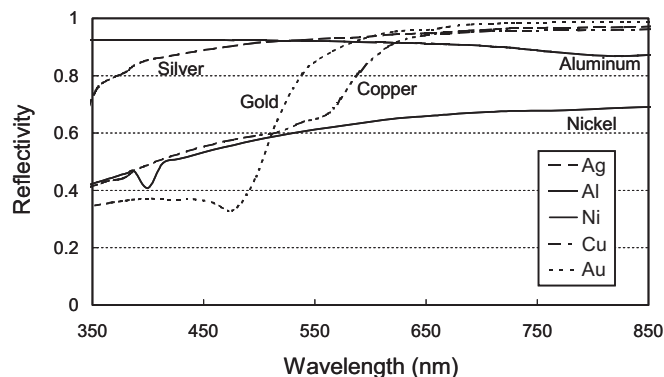


Figure 1. Reflectivity of metals from reference materials [19].

during the nickel plating process. Our group previously demonstrated the selective or non-selective electroless plating of self-assembled latex particle monolayers and polyelectrolyte multilayers (PEM) for opto-electronic applications.^[21,22a] Additionally, we have also shown that monodisperse functional particles can be adsorbed from colloidal solution onto oppositely charged PEM coated glass substrates.^[23] These particles form a unique self-assembled monolayer of random-close-packed (rcp) clusters whose formation is controlled by electrostatic and capillary forces. Since a uniformly plated particle monolayer is rough over a large area, we have investigated the possibility of using the surface as a diffuse reflector.

PEM are strong adhesive layers of functional polymers, which can deposit on metal, glass, and oxides surfaces.^[24] PEM do not affect to the optical properties of visible light due to their ultra thin film thickness. Using PEM also removes a need for expensive vacuum metal deposition techniques because PEM can be metallized with electroless plating.^[21,22a,25,26]

In our work, particle monolayers formed on PEM are coated with nickel in a two-step electroless plating method using palladium catalysts. A quartz crystal microbalance (QCM) is employed to study the kinetics and the catalyst effect of electroless nickel plating on PEM. A phase angle optical microscope and a scanning electron microscope are employed to physically characterize the surfaces. The optical properties of the diffuse reflector are characterized using a UV-VIS spectrometer with fiber optic cables. These fiber optic cables permit the sample reflectance to be measured at multiple angles. We demonstrate how to estimate the distribution of reflected light from the surface. Also, the ratio of specular and diffuse reflection in the total reflected light is quantified by measuring the angle dependent reflectance. Optical measurements of our diffuse reflectors prove the ease of controlling the reflection ratio by simply adjusting the particle size. This shows promising results for the potential application of our diffuse reflectors.

2. Results and Discussion

A QCM was used to measure the plating rates of different surface and catalyst combinations. Multilayers were created on

the surfaces of gold coated quartz sensors. First a carboxylic acid terminated self-assembled monolayer was created on the gold surface. Then the sensors were mechanically coated with (PDAC/SPS)₁₀ or (PDAC/SPS)_{10.5} bilayer PEM films. Some samples were then activated using a palladium catalyst. The six different surface types tested are listed in Table 1. Figure 2 shows the QCM measurements of electroless nickel plating rates on PEM. Nickel plating shows linear growth over time, without a saturation curve, due to the constant reaction of nickel plating. A PDAC or SPS surface without catalyst, C1 and C2

Table 1. Surface types of prepared samples.

Samples	Surface preparation
C1	PDAC without catalyst
C2	SPS without catalyst
C3	PDAC with catalyst I
C4	PDAC with catalyst II
C5	SPS with catalyst I
C6	SPS with catalyst II

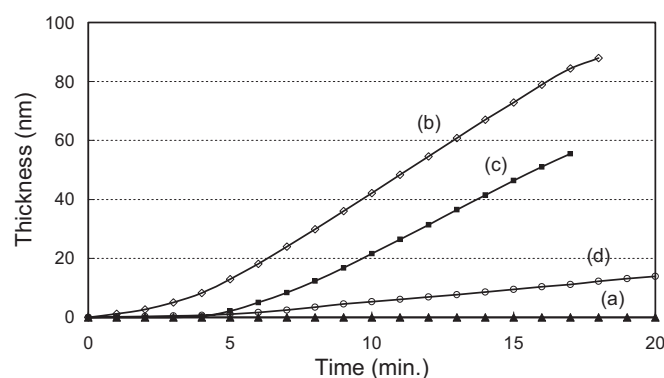


Figure 2. QCM Measurements. a) C1, C2, and C3. b) C4. c) C5. d) C6.

respectively, show no nickel reduction on the surface over long times. On the other hand, PDAC with the negatively charged catalyst on the surface, C4, shows the highest plating rate. The maximum thickness before delamination was estimated to be 88 nm. After about 15 minutes of plating, cracks were observed on the nickel surface. The whole metal layer delaminated from the QCM sensor at 18 minutes. A SPS surface activated with the positive catalyst, C5, also shows a high plating rate. However, the maximum thickness before delamination was only 55.5 nm which is less than the final thickness on PDAC, C4. These results show that for nickel to plate on PEM surface, a palladium catalyst is required. Also, the negative catalyst is more reactive than its positive counterpart.

A positive PDAC surface with the positive catalyst, C3, did not have any nickel growth. However, the negative SPS surface with the negative catalyst, C6, had some nickel deposited on the surface. This shows the non-selectivity of the negative cata-

lyst and suggests that some of the negative catalyst will deposit on the negatively charged particle surfaces during the catalyst loading step of the particle monolayer coated PEM surfaces.^[21] Dressick, et al., reported that PdCl_4^{2-} rapidly hydrolyzes in water forming bulk precipitations which may have also caused this behavior.^[27] Additionally, it suggests that the final layer of SPS does not completely cover the entire surface of the PDAC. This inexcusively adsorbed final SPS layer has also been observed in some of our selective nickel patterning data.^[22b]

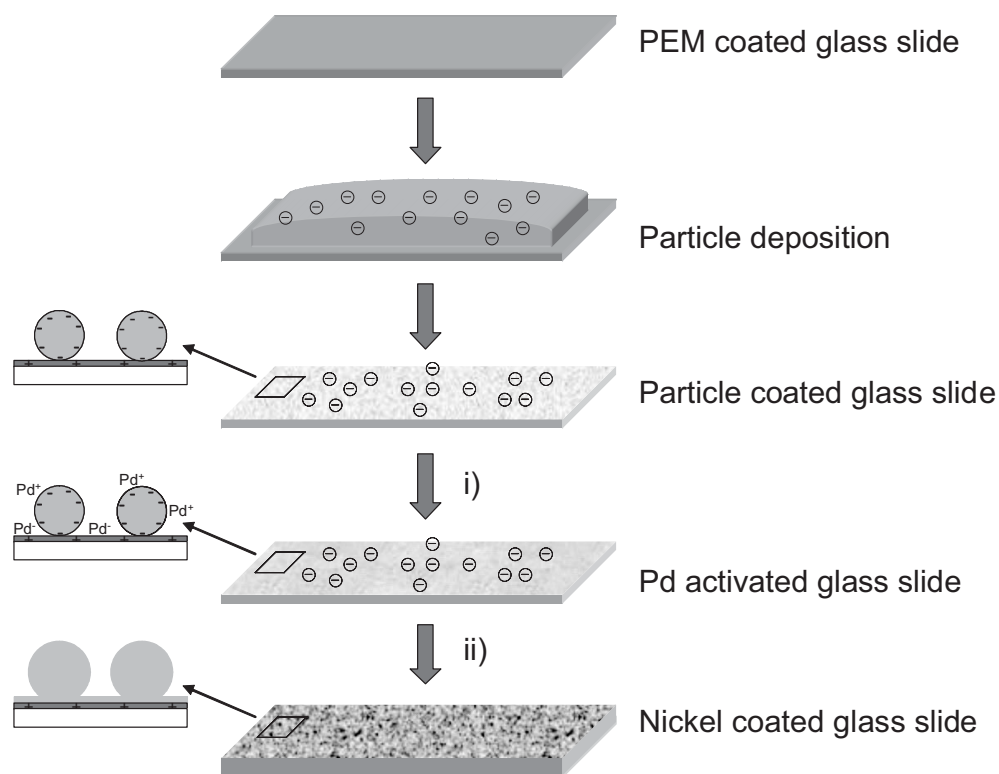
As shown in Scheme 1, we deposited self-assembled particle monolayers onto the PEM surface and then electrolessly plated the entire surface (particles and PEM) with nickel. Figure 3 shows microscope images of nickel-plated colloidal monolayers using 140 nm, 500 nm, and 3 μm particles. As studied in our earlier work, the nanospheres (~ 100 nm), shown in Figure 3A, are adsorbed independently and the like charge repulsion of the particles dominates their self-assembly during the drying step.^[23] During electroless plating, the thick nickel metal layer growing on the surface of the spherical particles and the substrate, results in the development of hemispherical and irregular shapes as observed in Figure 3A. The thickness of the deposited nickel was comparable to the diameter of nanospheres in the monolayer.

Figure 3B shows a nickel-plated colloidal monolayer using 500 nm sized particles. Different from the nanospheres ($D_{\text{particle}} \sim 100$ nm), microspheres ($D_{\text{particle}} > 0.5 \mu\text{m}$) develop branch-like structure clusters of particles due to the strong capillary force generated around the particles during monolayer

formation.^[23] Figure 3B shows that the nickel coated spherical particles kept their shape but occasionally two or more adjacent particles appeared to merge or aggregate due to necking. Heavy necking between particles is due to the growth of nickel on their surface.

Figure 3C shows a bright field optical microscopic image of a 3 μm particle monolayer. This figure is a clear demonstration of sources of specular and diffuse reflection. In the image bright color appear from the regions of particle top surfaces and nickel coated PEM surfaces without particles. These regions reflect light in a specular manner detectable in a bright filed detector. On the other hand, the curved side regions of the particles are dark showing the source of diffuse reflection. Note that light scattered diffusively is not detectable under bright field mode making the diffusive surfaces appear dark in the image. This image demonstrates that the more particles you can incorporate in the particle monolayer, the more diffuse reflection one can achieve. This aspect will be further discussed later in this paper.

As shown in Figure 3C, long electroless plating times develop crazes on the particle. As reported elsewhere, crazes and delamination are due to the internal stress build-up during electroless plating and have been a great limitation of the electroless plating process.^[28,29] For optical reflector applications, there should be little transmittance of light through the electrolessly formed reflectors. However, the electroless nickel plating of PEM coated substrates without particle monolayers did not create a large enough thickness to reduce the loss of



Scheme 1. Fabrication process to create nickel coated reflectors. In processes i) the samples are immersed in positively and negatively charged palladium catalyst solutions consecutively and ii) the samples are placed in the electroless deposition bath.

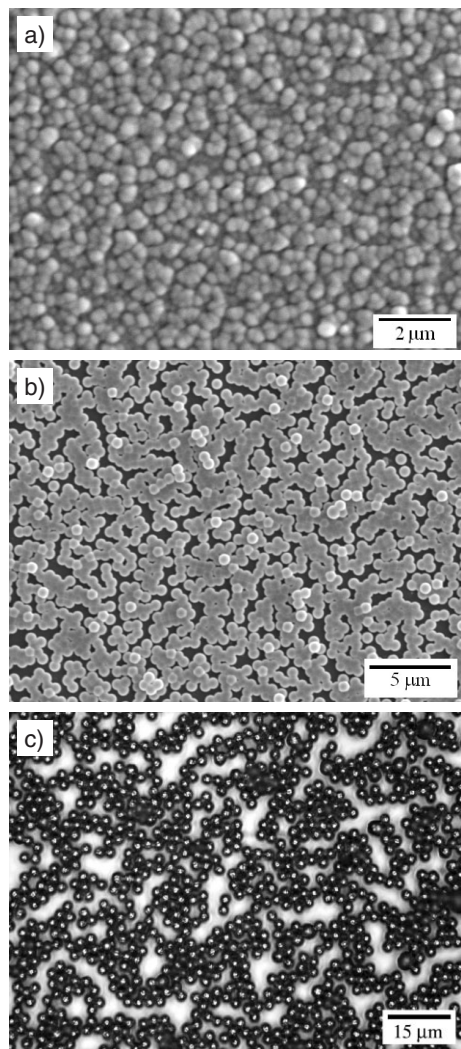


Figure 3. A) SEM image of 140 nm particles with nickel plating. B) SEM image of 500 nm particles with nickel plating. C) Brightfield microscopic image of 3 μm particles with nickel plating.

light from transmission. After a 30 minute plating time, the transmittance of particle coated samples, which was measured by an UV-vis spectrophotometer, showed no significant transmission of light.

Interestingly we also observed that nickel formed by electroless deposition on a rough (i.e., particle coated) surface can bear greater internal stress than on a smooth (PEM) surface under the same plating conditions. At around 15 minutes of plating the whole metal layer delaminates from a PEM surface without particles, while delamination does not occur on a particle monolayer coated surface for over 30 minutes. We believe that particles incorporated into the polymer-nickel interface plating break-up and deflect the internal stress in the electrolessly deposited nickel film. By deflecting these forces in a new direction the nickel layer is able to form a thicker layer than was possible without the particle monolayer.^[30] This al-

lows for interesting future work that focuses on strengthening mechanical properties by the incorporation of nanoparticles into the plating process.

In this study, the crazed surface of nickel scatters more light in a diffuse manner making it an excellent choice for diffuse reflector applications. However for other applications, when a thicker metal layer or composite multilayers are required, the plating rate, temperature, pH of bath solution, and selection of a different substrate for Ni plating should be optimized to lower the internal stress.^[28,29] Another modification, changing the type of polyelectrolytes used may change the type of interactions with the Pd catalyst and result in better adhesion to the metal and prevent delamination.^[31]

Figure 4 shows the average specular and diffuse reflectance as a function of particle size for samples that were nickel plated for 30 minutes. The average specular reflectance decreases and the average diffuse reflectance increases as particle size increases. The measured specular reflectance was referenced against a high specular standard, so the highest specular reflectance we recorded was 38.09 % for the 140 nm samples. The samples made of particles greater than 3 μm have values of specular reflectance less than 0.6 %. This result shows strong evidence that the electroless deposition technique can control surface morphology simply by changing the size of particle adsorbed on the substrates before plating.

Figure 5 shows the distribution of light reflected from the sample surfaces at different angles. This was performed by the integration of the angular dependent reflectance. When the incident angle is 5°, specularly reflected light is in between 0–3° on the graph. It turns out that the reflectors created using our method do not produce a focused reflection. Instead, the reflectors scatter light randomly in all directions. The reflected light distribution data was further analyzed and the ratio of the specular to diffuse reflection at the incident angle of 5° was derived and is shown in Table 2. The result shows that using our method the amount of specular reflection can be controlled between ~40 to 90 % by simply changing the size of the particles.

The portion of diffuse reflection in Table 2 converges at 60 % as we increase the particle size. For example, the portions

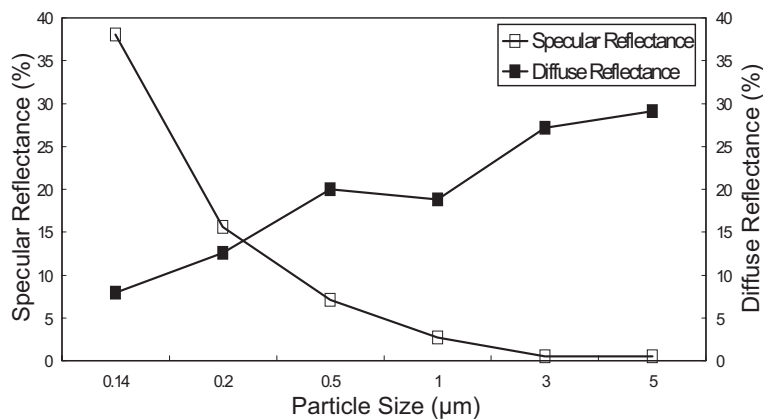


Figure 4. UV-VIS spectrometer measurements of the specular and diffuse reflectance of nickel coated particle monolayers on PEM.

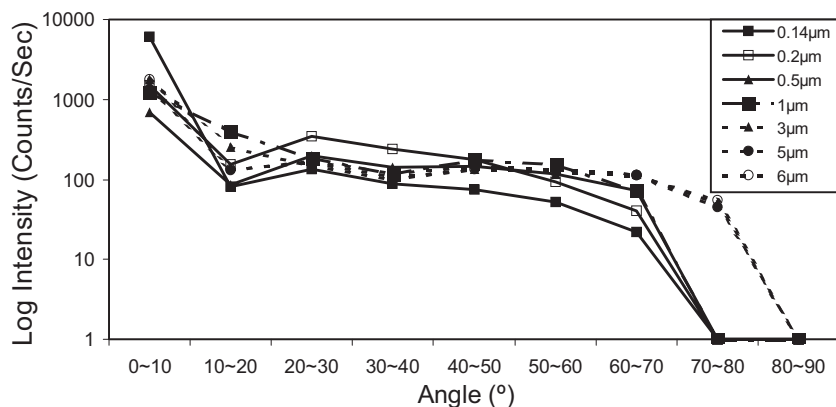


Figure 5. Angular distribution of reflected light from the rough nickel surface.

Table 2. Specular versus diffuse reflections as a function of particle size at the polymer-metal interfaces.

Particle size [μm]	0.14	0.2	0.5	1	3	5
Portion of specular reflection [%][a]	91.75	57.66	45.38	43.52	40.03	40.79
Portion of diffuse reflection [%][a]	8.25	42.34	54.62	56.48	59.97	59.21
Diffuse reflectance [%][b]	8	12.5	20	19	27	29

[a] Portion diffuse and specular reflection among total reflected light calculated from figure 5. [b] Diffuse reflectance in figure 4 with 75° of incident and 0° of detecting angle.

of diffuse reflection of 0.5 μm and 5 μm samples are 54.62 and 59.21%. So, 10 times change in particle diameter changed ~5% in the portion of specular/diffuse reflection. Note that similar portion of diffuse reflection doesn't mean that the optical properties are the same. Figures 4 and 6 demonstrate this fact, the 5 μm sample reflects light more broadly than 0.5 μm sample resulting in a wider viewing angle. In designing a reflector, the portion of specular/diffuse reflection and viewing angle

should both be taken into account. Table 2 provides a guide to select a particle size for desired optical properties of specific applications such as backlight unit.

When there is a need for reflectors with the portion of diffuse reflection more than 60%, our approach described in this paper should be modified. As we discussed earlier in this paper, diffuse reflection will increase with increase in particle coverage of the surface. Large areas without particles in Figure 3C should be filled with particles because they are sources of specular reflection. However, in rcp monolayers, increasing surface coverage of particle is not easy due to the electrostatic repulsive force between particles.^[23] Increasing the particle coverage of monolayer

will be an important future work in terms of creating more diffusive reflectors. An interesting future work which remains is filling the voids of rcp monolayers with the self-assembly of smaller particles to enhance the surface coverage.^[32]

Figure 6 shows two macroscopic images of the reflectors taken by a digital camera at different angles. In both images the particle size increases from left to right, and the far left sample is a particle free nickel reflector. The brightness of the specular reflection (upper half) inversely changes with an increase in particle size, however, the diffuse reflection (lower half) increases with particle diameter. Particle free or nanosphere monolayers (left side of figure) are brighter in specular reflection and darker in diffuse reflection than bigger particle monolayers (right side of figure). It is because the nanospheres (left) reflect most of the impinging light specularly as calculated in Table 2. On the other hand, samples with microspheres (right) are darker at specular reflection angles and brighter at the diffuse reflection angles because they reflect about half of the incident light specularly and the other half diffusively. These results, which are shown in Figure 6, agree with the measurements of specular and diffuse reflectance shown in Figure 4.

3. Conclusions

We have presented a novel fabrication method to produce diffuse reflectors that does not require a high vacuum or special equipment. Tuning the specular and diffuse reflectance has been easily achieved by simply changing the particle size. In addition, a self-assembled monolayer of particles at the interface enhanced the adhesion of polymer and metal and allowed for a greater metal film thickness before delamination. The presented method is cost-effective and convenient for mass production because the process consists of a series of simple immersion steps.

The UV-vis spectrophotometer with optical fibers was used for various combinations of incident and detecting angles resulting in versatile measurements of the specular and diffuse reflectance. The spectrophotometer could also measure the angular dependent reflectance without any expensive devices.

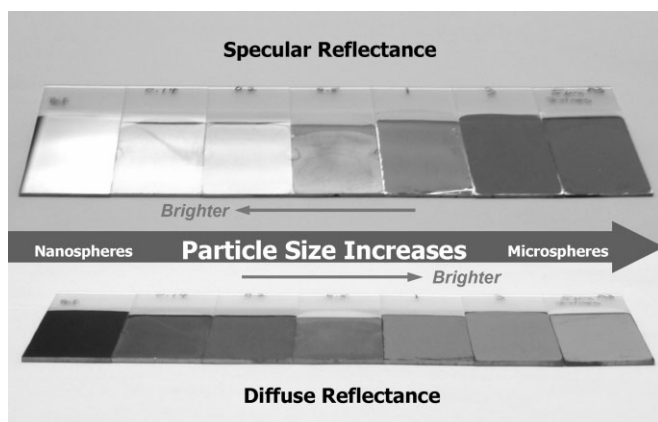


Figure 6. Side by side comparison of the specular and diffuse reflectance of nickel coated particle monolayers on PEM coated substrates.

Angular dependent measurements and simple integration successfully demonstrated how to derive the distribution of reflected light and the ratio of the specular to diffuse reflectance in the total reflected light.

The portion of specularly reflected light from the total reflected light ranged from 40–90% as a function of particle size. To decrease specular reflection or increase diffuse reflection further, additional modifications are required. Additional modifications include higher concentrated self-assembled monolayer, using two differently sized particles^[32] or a rougher outer metal coating. Increasing particle density by the use of a surfactant or the multilayering of other metals remains as future work. The stability or durability of the prepared metal-polymer reflectors also remains for future investigation. We believe this study opens a way to fabricate more complex systems fabricated from PEM, particle monolayers and electroless deposition.

4. Experimental

Materials: Poly(diallyldimethylammonium chloride) (PDAC) and sulfonated polystyrene (SPS) were purchased from Aldrich (Milwaukee, WI). Average molecular weights of PDAC and SPS are ~100 000–200 000 and 70 000, respectively. For electroless plating, Nickel sulfate, sodium citrate dihydrate, lactic acid, Tetraamminepalladium(II) Chloride monohydrate ($\text{Pd}(\text{NH}_4)_4\text{Cl}_2$), and borane-dimethylamine complex (DMAB) were ordered from Aldrich and Sodium tetrachloropalladate(III) trihydrate (Na_2PdCl_4) was purchased from Strem chemicals (Newburyport, MA). 16-mercaptodecanoic acid was also ordered from Aldrich. Glass microscope slides were ordered from Corning (Corning Glass Works, Corning, NY) and used as transparent substrates for polyelectrolyte multilayer and particle coatings. All aqueous solutions in the process were created with deionized (DI) water (>18.1 M Ω) which was supplied by a Barnstead Nanopure Diamond-UV purification unit equipped with a UV source and a final 0.2 μm filter.

Polyelectrolyte Multilayer Formation: Glass slides were first cleaned with an ultrasonic unit containing a commercially available detergent (Alconox, Inc.) in aqueous solution for 20 min to degrease the samples. Then the samples were cleaned a second time with the same ultrasonic unit in DI water without detergent for 10 min. The glass slides were dried under an N_2 gas stream. Then they were treated with oxygen plasma for 10 min at 150 mTorr vacuum for further cleaning and the activation of the negative surface charges on glass. Aqueous solutions of 20 mM PDAC and 10 mM SPS were prepared, each containing 0.1 M NaCl. Polymer concentrations are based on the molecular weight of the repeat unit. Alternating layers of PDAC/SPS were fabricated by sequential immersion into the solutions using a Microm DS 50 Slide Stainer purchased from Richard-Allan Scientific (Kalamazoo, MI). The first polyelectrolyte deposited on the glass surface was PDAC that has positively charged ammine groups which are attracted to the negatively charged hydroxyl groups on glass. Glass slides were immersed into PDAC aqueous solution for 20 min followed by two rinsing steps with DI water for 5 min each. The samples were then immersed into SPS solution for 20 min, and then followed by another two rinsing steps. The substrates then were immersed into an ultrasonic bath for 1 min removing loosely attached polyelectrolyte. This loop of immersion steps creates 1 bilayer of PDAC and SPS and was repeated until (PDAC/SPS)_{10.5} bilayers films were formed. (PDAC/SPS)_{10.5} bilayers have PDAC top surface. After film formation, substrates were finally dried under an N_2 gas stream and stored for further modification.

Self-Assembled Particle Monolayers: Six different sized sulfate and carboxylic acid functionalized particles were used, with particle diameters ranging from 100 nm to 5 μm . Sulfate polystyrene particles were ordered from Interfacial Dynamics Corp. and carboxylate polystyrene

particles were ordered from Polysciences, Inc. For more details on the particles see our previous work [23]. Colloidal solutions were diluted to 0.5 wt% from their initial concentration. For particle deposition onto the PEM, we pipetted small amounts of the colloidal particle solution onto the PEM coated substrate and waited for about 1 h to permit full adsorption. Then the particle-coated substrates were washed carefully with DI water and dried under an N_2 stream.

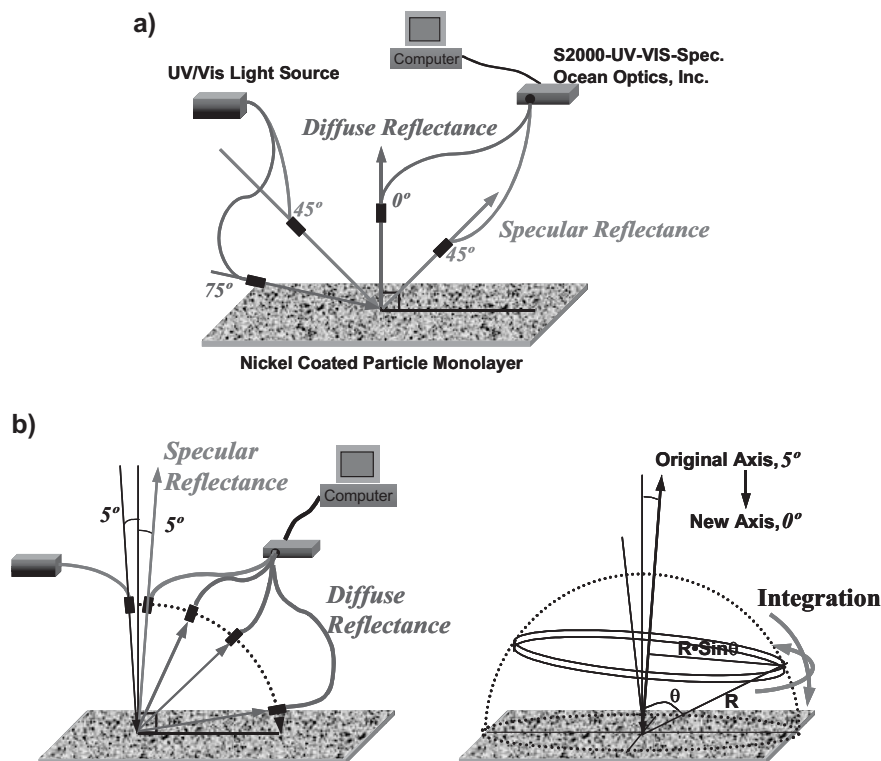
Electroless Plating of Self-Assembled Particle Monolayers: Two Pd based catalyst solutions were prepared using $\text{Pd}(\text{NH}_4)_4\text{Cl}_2$ (catalyst 1) and Na_2PdCl_4 (catalyst 2), each with a 5 mM concentration in DI water. The samples of 2D colloidal monolayers were immersed into the two freshly prepared catalyst solutions in succession for 10 s in each bath (step 1). After washing with DI water followed by N_2 drying, the activated samples were dipped into a Ni bath (step 2) for 30 min. The electroless nickel bath contained nickel sulfate (Ni source, 4 g), sodium citrate (complexant, 2 g), lactic acid (buffer, complexant, 1 g), and DMAB (reductant, 0.2 g) in 100 ml of DI water. The pH of the Ni bath was adjusted to 6.5 ± 0.1 using ammonium hydroxide. For a particle free nickel surface, a similar electroless plating method was applied to a polyelectrolyte coated substrate without a particle monolayer. Particle free nickel surfaces were grown from either a PDAC or SPS topped surface which were loaded with either a negative or positive catalyst, respectively. Scheme 1 summarizes the fabrication of reflectors from PEM deposition to nickel plating.

Quartz Crystal Microbalance Measurement: The rate of electroless plating was measured utilizing a research quartz crystal microbalance (QCM) manufactured by Maxtek, Inc. (Santa Fe Springs, CA). Gold-coated polished 5 MHz QCM sensors were ordered from the same company. Sensor surfaces were cleaned with plasma treatment for 2 min and immersed over night into a 1 mM solution of 16-mercaptodecanoic acid. (PDAC/SPS)₁₀ and (PDAC/SPS)_{10.5} bilayers of PEM were coated on the carboxylic acid terminated thiol surface. 6 different PEM surfaces, summarized in Table 1, were prepared for QCM measurements. If the PEM surface was activated with a catalyst, the QCM sensor was immersed in the catalyst for 10 seconds before rinsing with water. QCM measurements were performed using the same nickel bath described above at room temperature.

Characterization: Microscopic images of the particle monolayers on PEM surfaces were obtained using an optical microscope (Nikon Eclipse ME600) and a Scanning Electron Microscope (JEOL 6400V with a LaB_6 emitter). To study the optical properties of the samples, a USB2000 spectrometer from Ocean Optics was employed. This spectrometer is unique because both the light source and detector can be connected with movable fiber optic cables. All specular and diffuse reflectance spectra of the samples were referenced against high specular and diffuse reflectance standards purchased from Ocean Optics.

Scheme 2a shows the measurement schematic for the specular and diffuse reflectance. The probing beam diameter was 0.5 cm. For all measurements, a distance of 30 cm was maintained between the end of the light source optical fiber and the sample. Similarly, the same distance was maintained between the sample and the detecting optical fiber. To measure the specular reflectance the light source and the detecting probe are placed on opposite sides. Both the incident and detecting angles were 45° from the surface normal. For diffuse reflectance the incident angle was 75° and the detecting angle was 0° . Collimation of the optical fibers was checked by disconnecting optical fiber from the light source and shining strong red laser through the optical fibers. The ends of the optical fibers were carefully moved until the strong red light signal is detected. Reflectance spectra were then averaged over the visible light range (400–500 nm) and reported as a single value. Data collected using this method is displayed in Figure 4.

Scheme 2b shows the schematic for measuring a distribution of light reflected from the sample surface. The incident angle was 5° to the surface normal and the mobile detecting probe was placed at different reflection angles between 5° and 90° to acquire the angular dependent reflectance. To hold and move the ends of the optical fiber connected to the detector, a rotation stage with attached protractor was built in-house. All reflectance intensities (i.e., number of photon per unit time) were measured at different angles, and averaged across the visible light range. Average values were divided by the detector area resulting in



Scheme 2. A) Optical measurement scheme for specular and diffuse reflectance. B) Optical measurement scheme for distribution of reflected light.

flux density (i.e., number of photons per unit time and area). The flux densities at each angle were multiplied by the area calculated from the integration of an imaginary sphere at a given angle range. Once multiplied by the area, the flux densities were converted to flux (i.e., number of photons per unit time) and integration assumed that the distribution of light was hemispherical because the incident angle was close to 0°. Equation 1 was used in the integration as follows:

$$\text{Reflectance} = \frac{\text{intensity}}{\text{time area}} \int_{\theta_1}^{\theta_2} 2\pi R^2 \sin \theta d\theta \quad (1)$$

Where R is the radius of the hemisphere, and θ_1 and θ_2 are the angles in the given range. This resulted in intensity as shown in Figure 5. The ratio of specularly and diffusively reflected light was derived from the distribution of the reflected light. It was assumed that the specularly reflected light from the surface was populated in the region between a 0–3° reflecting angle when incident light impinged the surface at an angle of 5°. The area of the region in between the reflecting angle 0–3° on the imaginary hemisphere was equivalent to that of the detector.

To compare the brightness from a macroscopic view of the reflectors, a Nikon digital camera and Xenon KX2000 fluorescent light bulb were employed. The reflectors were placed on a white paper covered desk and photographed at the incident angle of 45° and detecting angle of 45° and 75° for to observe the specular and diffuse reflectance, respectively.

Received: March 2, 2007

Revised: May 9, 2007

Published online: October 23, 2007

[1] C.-k. Wei, in *U.S.*, (Industrial Technology Research Institute, Taiwan). US 5595790, **1997**, p. 7.
 [2] W. D. Kretzman, S. R. Kaytor, in *U.S.*, (3M Innovative Properties Company, USA). US, **2002**, pp. 28.
 [3] M. Sakamoto, Y. Yamaguchi, H. Ikeno, F. Matsuno, H. Kikkawa, in *Eur. Pat. Appl.*, (NEC Corporation, Japan). EP 1237016, **2002**.
 [4] S. H. Lee, T. H. Yoon, J. C. Kim, *Opt. Lett.* **2006**, *31*, 2196.
 [5] Y. J. Lee, H. C. Kuo, T. C. Lu, S. C. Wang, *IEEE J. Quantum Electron.* **2006**, *42*, 1196.
 [6] Y. Xi, X. Li, J. K. Kim, F. Mont, T. Gessmann, H. Luo, E. F. Schubert, *J. Vac. Sci. Technol. A* **2006**, *24*, 1627.
 [7] A. Banerjee, S. Guha, *J. Appl. Phys.* **1991**, *69*, 1030.
 [8] J. E. Cotter, *J. Appl. Phys.* **1998**, *84*, 618.
 [9] P. A. Fedders, *Phys. Rev.* **1969**, *181*, 1053.
 [10] R. Fuellemann, R. Mauser, M. Specht, H. Stauch, D. Oelkrug, *J. Mol. Struct.* **1986**, *143*, 251.
 [11] C. S. West, K. A. O'Donnell, *Phys. Rev. B* **1999**, *59*, 2393.
 [12] A. Roos, M. Bergkvist, C. G. Ribbing, J. M. Bennett, *Thin Solid Films* **1988**, *164*, 5.
 [13] K. Kamoshida, *J. Vac. Sci. Technol. B* **2000**, *18*, 2565.
 [14] N. D. Nikolic, Z. Rakocevic, K. I. Popov, *J. Electroanal. Chem.* **2001**, *514*, 56.
 [15] N. D. Nikolic, Z. Rakocevic, D. R. Durovic, K. I. Popov, *J. Serb. Chem. Soc.* **2002**, *67*, 437.

[16] Q. C. Zhang, D. R. Mills, *J. Appl. Phys.* **1992**, *72*, 3013.
 [17] A. B. Dimant, I. E. Belinovich, L. S. Tuzov, V. M. Kolotykin, V. P. Fedorenko, Y. V. Egorov, *Fr. Demande*, Scientific-Research and Experimental Institute of Motor-Vehicle Electrical Equipment and Instruments, USSR, FR 2476142, **1981**, p. 19.
 [18] H. Okitsu, *Jpn. Kokai Tokkyo Koho* JP 11134912 **1999**, 5.
 [19] D. R. Lide, *CRC Handbook of Chemistry and Physics*, 71st ed., CRC Press, Boca Raton, FL **1991**.
 [20] W. R. Veazey, *Handbook of Chemistry and Physics*, 57th ed., Chemical Rubber Pub. Co., Cleveland **1976/77**.
 [21] I. Lee, P. T. Hammond, M. F. Rubner, *Chem. Mater.* **2003**, *15*, 4583.
 [22] a) T. R. Hendricks, I. Lee, *Thin Solid Films* **2006**, *515*, 2347. b) T. R. Hendricks, E. E. Dams, S. T. Wensing, I. Lee, *Langmuir* **2007**, *23*, 7404.
 [23] J. S. Ahn, P. T. Hammond, M. F. Rubner, I. Lee, *Colloids Surf. A* **2005**, *259*, 45.
 [24] P. T. Hammond, *Adv. Mater.* **2004**, *16*, 1271.
 [25] T. C. Wang, B. Chen, M. F. Rubner, R. E. Cohen, *Langmuir* **2001**, *17*, 6610.
 [26] T. C. Wang, R. E. Cohen, M. F. Rubner, *Adv. Mater.* **2002**, *14*, 1534.
 [27] W. J. Dressick, C. S. Dulcey, J. H. Georger, G. S. Calabrese, J. M. Calvert, *J. Electrochem. Soc.* **1994**, *141*, 210.
 [28] J. Y. Song, J. Yu, *Thin Solid Films* **2002**, *415*, 167.
 [29] N. M. Martyak, *Met. Finish.* **2003**, *101*, 41.
 [30] T. R. Hendricks, I. Lee, *Nano Lett.* **2007**, *7*, 372.
 [31] M. S. Chen, C. S. Dulcey, S. L. Brandow, D. N. Leonard, W. J. Dressick, J. M. Calvert, C. W. Sims, *J. Electrochem. Soc.* **2000**, *147*, 2607.
 [32] H. Takei, *J. Vac. Sci. Technol. B* **1999**, *17*, 1906.